Digital Communications and Networks 8 (2022) 303–313

Contents lists available at ScienceDirect

Digital Communications and Networks

journal homepage: www.keaipublishing.com/dcan

Simultaneous wireless information and power transfer with fixed and adaptive modulation

Jie Hu [a], Guangming Liang [b], Qin Yu [a,*], Kun Yang [b], Xiaofeng Lu [c]

[a] Yangtze Delta Region Institute (Huzhou) & School of Information and Communication Engineering, University of Electronic Science and Technology of China, Huzhou, 313001, China
[b] School of Information and Communication Engineering, University of Electronic Science and Technology of China, Chengdu, 611731, China
[c] State Key Laboratory of Integrated Services Networks, Xidian University, Xi'an, 710071, China

ARTICLE INFO

Keywords:
Simultaneous wireless information and power transfer (SWIPT)
Fixed/adaptive modulation
Rate-energy-reliability trade-off
Transceiver design
Energy self-sustainability

ABSTRACT

Activating Wireless Power Transfer (WPT) in Radio-Frequency (RF) to provide on-demand energy supply to widely deployed Internet of Everything devices is a key to the next-generation energy self-sustainable 6G network. However, Simultaneous Wireless Information and Power Transfer (SWIPT) in the same RF bands is challenging. The majority of previous studies compared SWIPT performance to Gaussian signaling with an infinite alphabet, which is impossible to implement in any realistic communication system. In contrast, we study the SWIPT system in a well-known Nakagami-m wireless fading channel using practical modulation techniques with finite alphabet. The attainable rate-energy-reliability tradeoff and the corresponding rationale are revealed for fixed modulation schemes. Furthermore, an adaptive modulation-based transceiver is provided for further expanding the attainable rate-energy-reliability region based on various SWIPT performances of different modulation schemes. The modulation switching thresholds and transmit power allocation at the SWIPT transmitter and the power splitting ratios at the SWIPT receiver are jointly optimized to maximize the attainable spectrum efficiency of wireless information transfer while satisfying the WPT requirement and the instantaneous and average BER constraints. Numerical results demonstrate the SWIPT performance of various fixed modulation schemes in different fading conditions. The advantage of the adaptive modulation-based SWIPT transceiver is validated.

1. Introduction

1.1. Background

Internet of Everything (IoE) is one of the key 6G applications for smart cities [1]. Many IoE devices for sensing and communications are being massively deployed around every corner. However, the limited battery capacity of these miniature devices substantially constrains their lifetime, which may heavily impair network functions and substantially increase the maintenance cost for replacing drained batteries. Harvesting ambient energy from the environment may relieve IoE devices from the constraints of limited battery capacity [2]. However, it primarily relies upon the unpredictable environment. The intermittent energy supply cannot ensure the Quality of Service (QoS) of the sensing and communications of IoE devices.

Consequently, active Wireless Power Transfer (WPT) is needed for providing controllable and on-demand energy supply to a rechargeable battery or batteryless powered IoE devices. Radio Frequency (RF) signal-based WPT is more suitable in the scenario of IoE than inductive coupling [3] and magnetic resonance [4] based methods for the following reasons:

- IoE devices are deployed in the far field of transmitters. Inductive coupling and magnetic resonance based WPT can only deliver energy to devices centimeters away from transmitters. However, by radiating RF signals, wireless power can be delivered more than tens of meters away.
- IoE devices are extensively deployed in a certain region. RF signals transmitted by multiple antennas may flexibly form either narrow beams for high-energy point-to-point WPT, or wide beams for wireless power multicast toward multiple devices. However, inductive coupling and magnetic resonance are limited for point-to-point WPT.
- There are many RF transmitters such as cellular Base Stations (BSs), WiFi Access Points (APs), and TV towers. By exploiting legacy

* Corresponding author.
E-mail addresses: hujie@uestc.edu.cn (J. Hu), lianggm@std.uestc.edu.cn (G. Liang), yuqin@uestc.edu.cn (Q. Yu), kunyang@uestc.edu.cn (K. Yang), luxf@xidian.edu.cn (X. Lu).

https://doi.org/10.1016/j.dcan.2022.01.001
Received 20 January 2021; Received in revised form 29 December 2021; Accepted 12 January 2022
Available online 19 January 2022

infrastructure, we do not require dedicated equipment for providing WPT services.

Coordinating WPT services along with conventional Wireless Information Transfer (WIT) services results in many challenges in the design of the physical layer, medium-access-control layer, and networking layer, which stimulate substantial interest in relevant research of Simultaneous Wireless Information and Power Transfer (SWIPT) and Integrated Data and Energy Networks (IDENs) [5]. Moreover, the future 6G network is envisioned to be energetically self-sustainable [6]. WPT will be considered a new service class as important as communication, computing, and sensing, while infrastructure and IoE devices in energy self-sustainable networks will operate in a super energy-efficient manner. Integrating WPT services in future 6G networks requires a holistic system design in every layer. Our study makes the first attempt to integrate both WIT and WPT services by designing practically modulated RF signals.

Although RF signals are capable of carrying wireless power to far-field IoE devices, the WPT still suffers from low efficiency, which results in a limited transmission range (15 m) [5]. Therefore, SWIPT should be exploited in some typical scenarios and integrated with other potential techniques. For example, it can be exploited for powering miniature IoE devices in some indoor scenarios, such as sensors in smart homes and smart factories. Therefore, SWIPT can be integrated with WiFi access points and indoor base stations for broadcasting downlink information and remotely charging these battery-powered and batteryless devices [7]. Moreover, SWIPT can also be integrated with Unmanned Aerial Vehicles (UAVs) to simultaneously collect data from IoE devices deployed in wide areas for environment monitoring, as UAVs may flexibly reduce their distance to batteryless devices to increase the efficiency of WPT [8].

1.2. Related works

By assuming that the transmit signal is also Gaussian distributed, the classic Shannon-Hartely capacity was calculated for characterizing the performance limit of WIT services in Additive-White-Gaussian-Noise (AWGN) channels. It is a common assumption in SWIPT [9–15].

Clerckx et al. [9] investigated a multi-sinusoidal based waveform design for SWIPT at the physical layer, which could be easily integrated with traditional Orthogonal-Frequency-Division-Multiplexing (OFDM)--based waveforms. Buckley et al. [10] exploited the cyclic prefix for dedicated WPT, while the other OFDM symbols were invoked for WIT. The Shannon-Hartely capacity was determined to evaluate the WIT performance of both [9,10]. Dai et al. [11] studied a millimeter-wave massive MIMO-based Non-Orthogonal-Multiple-Access (NOMA) system for SWIPT. Hybrid precoding was optimally designed by considering Gaussian signalling. Yue et al. [12] investigated the optimal transceiver design for simultaneous wireless information and power multicast in a multi-user millimeter-wave MIMO system by considering a limited number of RF chains and limited resolution of analog phase shifters. By assuming Gaussian signaling, the wireless information multicast performance was measured as the minimum spectral efficiency across all information users.

In the medium-access-control layer, Lv et al. [13] optimized downlink and uplink resources in the time-domain for supporting multiple batteryless devices in another energy-self-sustainable communication system, where both the sum-throughput and the fair-throughput were evaluated by assuming Gaussian signalling. Furthermore, Zhao et al. [14] proposed an enhanced carrier-sensing-multiple-access protocol for a SWIPT-based wireless local area network, and they studied an optimal deployment of a hybrid access point for delivering SWIPT services in Ref. [15].

Unfortunately, Gaussian-distributed signals cannot be actually generated, when a practical modulation scheme possessing finite alphabet is adopted. Therefore, we investigated the SWIPT performance of non-Gaussian distributed RF signals. Some pioneering works have initially discussed the influence of practical modulation schemes on the SWIPT performance [16–21]. For example, the rate-energy tradeoff was first discussed in Ref. [16] by considering discrete modulated symbols. The optimal precoder was optimally designed by Zhu et al. for SWIPT with practical modulation schemes in both [17,18], where the WIT performance was evaluated by the mutual information of discrete-input-continuous-output channels. Hu et al. [19] delivered a comprehensive guideline for modulation and coding design for SWIPT. Then, asymmetric phase-shift-keying was proposed in Ref. [20] for achieving the optimal SWIPT performance. Moreover, Zhao et al. [22] studied the SWIPT performance by invoking a receive spatial modulation, which substantially reduced the demodulation complexity at low-power IoE devices. Furthermore, a constellation rotation-aided modulation design was proposed for a non-orthogonal-multiple-access aided downlink SWIPT system in Ref. [21]. However, none of the above mentioned references revealed the rationale behind the SWIPT service delivery with practical modulation schemes. They all ignored the rate-energy-reliability tradeoff in the modulation design for SWIPT. To fill this gap, our previous work [23] originally investigated the rate-energy-reliability tradeoff by jointly optimizing a fixed modulation-based SWIPT transceiver.

Moreover, different modulation schemes have different Bit-Error-Ratio (BER) and Spectrum Efficiency (SE) performances. As a result, adaptively choosing a modulation scheme in a certain channel condition may achieve a better BER/SE performance overall. This is well known as an adaptive modulation [24]. According to Refs. [19,21], various WPT performances can be achieved by different modulation schemes in various channel conditions when non-linear energy harvesters are considered. However, none of the existing works consider the adaptive modulation for SWIPT.

1.3. Novel contributions

Against this background, our novel contributions are summarized as follows:

- We study a SWIPT system. The SWIPT transmitter conceives a practical digital modulator by adopting either a fixed or adaptive modulation scheme, and a buffer for storing the modulated symbols. With the aid of the buffer, reliable WIT can be guaranteed. The SWIPT receiver is batteryless. Its information demodulation is powered by the energy harvested from the downlink WPT service. It also harvests additional energy to power its other functions.
- We reveal the rationale behind the SWIPT service delivery with practical modulation schemes. We characterize the influence of different modulation schemes on the SWIPT performance in a Nakagami-m fading channel while evaluating the rate-energy-reliability tradeoff in various wireless fading conditions.
- For a fixed modulation-based SWIPT transceiver, we jointly optimize the transmission power and the transmission switching threshold at the SWIPT transmitter and the power splitting ratio at the SWIPT receiver to maximize the spectrum efficiency of the WIT service while satisfying the receiver's WIT reliability and WPT requirements.
- For an adaptive modulation-based SWIPT transceiver, we jointly optimize the modulation switching thresholds at the SWIPT transmitter and the power splitting ratio at the SWIPT receiver to maximize the average spectrum efficiency of the WIT while satisfying the receiver's instantaneous and average WIT reliability, as well as the energy-harvesting requirement.

The rest of the paper is organized as follows. Our system model is introduced in Section 2, while a fixed modulation-based SWIPT transceiver is optimized in Section 3, followed by the optimization of an adaptive modulation-based SWIPT transceiver in Section 4. After

providing numerical results in Section 5, we finally provide the conclusion in Section 6.

2. System model

In this section, we establish the influence of different modulation schemes on the SWIPT performance followed by the description of the transceiver architecture.

2.1. Modulation for SWIPT

Modulation is essential for practical communication systems, which modulates information RF signal amplitudes, phases, and frequencies. In this study, we mainly focus on amplitude- and phase-based modulation schemes. As shown in Fig. 1, the WIT capability of a modulation scheme is normally described by its constellation in an in-phase-quadrature coordinate. Nodes in a constellation represent all possible modulated symbols. The square of the Euclidean distance from the origin to a specific node represents the power carried by the corresponding modulated symbols. Having more nodes in a constellation represents that a single modulated symbol may carry more information bits, which results in higher spectrum efficiency. Furthermore, the minimum Euclidean distance between all pairs of nodes in a constellation represents the reliability of a modulation scheme. A higher minimum Euclidean distance of a specific modulation scheme relates to higher reliability. Fig. 1 outlines several classic modulation schemes, where we assume that all modulated symbols have equal probabilities to be sent, and the average power of all the modulated symbols is the same for different modulation schemes. As shown in Fig. 1(a), the Quadrature Amplitude Modulation (QAM) with an order of four (4-QAM) has a lower spectrum efficiency than 16-QAM. However, 4-QAM is much more reliable than 16-QAM. As shown in Fig. 1(b), 16-QAM, 16-Phase-Shift-Keying (16-PSK), and 16-Pulse-Amplitude-Modulation (16-PAM) have the same order. However, 16-QAM is the most reliable modulation scheme.

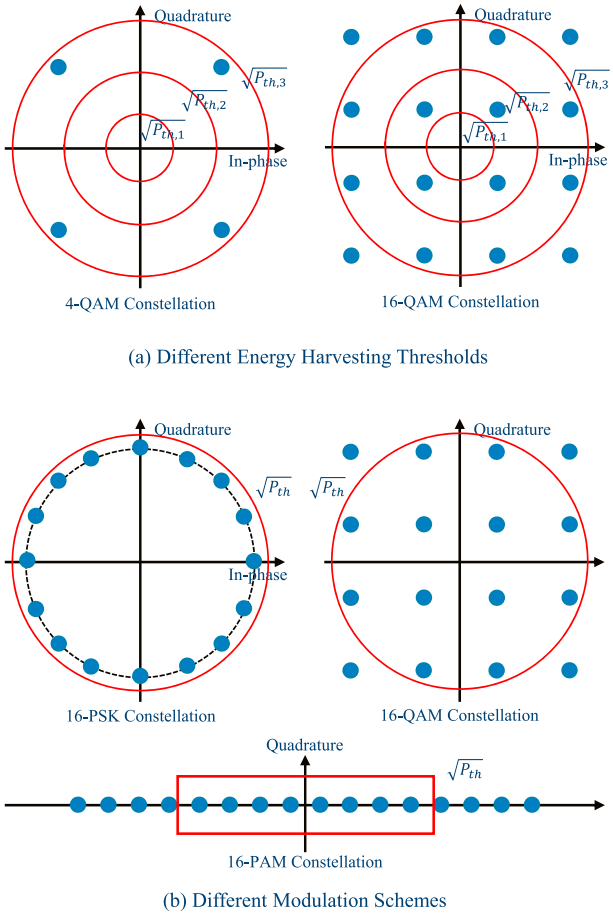

Fig. 1. Influence of different modulation schemes on SWIPT performance.

Furthermore, different modulation schemes have diverse WPT performances. As shown in Fig. 2, a SWIPT receiver has an information demodulator and an energy harvester. However, the energy harvested has to power the information demodulator. We assume that the minimum energy required by all functional modules of the SWIPT receiver is P_{th}. This indicates that only when the total energy harvested is higher than P_{th}, the battery can be effectively recharged. The WPT capability of a modulation scheme depends on how many modulated symbols carrying power are higher than P_{th}. As shown in Fig. 1(a), when we have a lower threshold $P_{th,1}$, the WPT performance of 4-QAM is higher than that of 16-QAM. However, as we increase the threshold to $P_{th,3}$, 4-QAM is outperformed by 16-QAM in terms of WPT performance. Furthermore, as shown in Fig. 1(b), given a common threshold to P_{th}, 16-PAM has the most modulated symbols carrying higher power than P_{th}. Therefore, it has the highest WPT performance. All the modulated symbols of 16-PSK carry lower power than P_{th}. As a result, they cannot be exploited for WPT.

Since different modulation schemes have various SWIPT performances, we have to design the SWIPT transceiver by considering these distinctive characteristics.

2.2. Transceiver architecture

Our SWIPT transceiver is illustrated in Fig. 2. The following modules constitute the SWIPT transmitter equipped with a single antenna:

- *Information Source* generates information bits requested by the SWIPT receiver.
- *The buffer* stores the information bits that need to be transmitted in the wireless medium. The information bits may output to the digital modulator when a certain channel condition can be achieved to guarantee the WIT's Quality of Service (QoS). Otherwise, they are pending to be transmitted in the buffer.
- *Digital Modulator* modulates information bits onto amplitudes and phases of RF signals by adopting either a fixed modulation scheme or an adaptive one. For a fixed modulation scheme, the digital modulator only operates when a certain channel condition satisfies the basic Bit-to-Error-Ratio (BER) requirement. For an adaptive modulation scheme, the digital modulator may adaptively switch among different modulation schemes to increase the attainable spectrum efficiency while satisfying both the BER requirement on the WIT and the energy harvesting requirement on the WPT.
- *Baseband to Passband* converts the modulated baseband signals to passband to transmit in wireless fading channels.

We consider an uncorrelated block fading wireless channel. The channel

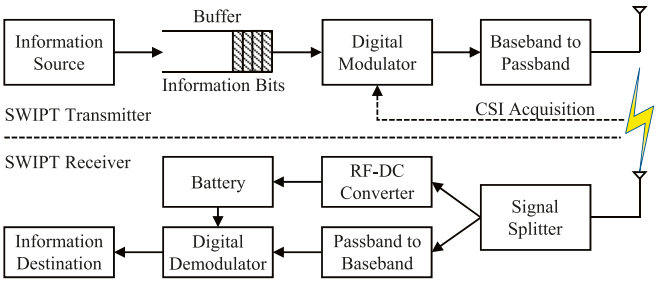

Fig. 2. SWIPT transceiver architecture.

amplitude coefficient, h, does not change within a symbol duration, but it varies from one symbol duration to another. We assume that the channel amplitude coefficient, h, follows a Nakagami-m distribution because it is feasible for modelling various fading conditions. Therefore, the corresponding channel power coefficient $v = |h|^2$ follows a Gamma distribution with parameter m, whose probability density function (pdf) is given by

$$f(v) = \frac{v^{m-1} m^m \exp(-mv)}{\Gamma(m)} \tag{1}$$

for $\forall m = 1, 2, \cdots$ [25]. In Eq. (1), m represents the channel fading factor. When $m = 1$, it is equivalent to a Rayleigh fading channel without any Line of Sight (LoS). A higher m indicates a less fading channel with a stronger LoS. For the channel attenuation incurred by the path loss, we have the distance, d, between the SWIPT transmitter and receiver while the path loss exponent is λ. The reference distance for path loss is $d_0 = 1$ m.

The SWIPT receiver comprises the following modules:

- *Signal Splitter* splits the received RF signals into two portions in the power domain. The first portion is used for energy harvesting and the second portion is used for information demodulation.
- *RF-DC Converter* converts the alternative current carried by a portion of RF signal to the Direct Current (DC), which can be used for recharging batteries and powering information demodulators.
- *Battery* is recharged by the DC, which completes the energy harvesting process. The actual energy harvested in the battery should exclude energy consumed for powering other functional modules.
- *Passband to Baseband* converts a portion of received passband RF signal to the baseband for processing in the digital domain.
- *Digital Demodulator* demodulates the baseband signal for extracting the information.
- *Information Destination* finally receives the demodulated information.

We assume that the SWIPT transmitter has sufficient knowledge of channel state information.

3. Transceiver optimization for fixed modulation

In this section, we firstly analyze the spectrum efficiency, BER, and energy harvesting performance of a fixed modulation-based SWIPT transceiver. Then, an optimal transceiver design is obtained for the sake of achieving a balance among these conflicted performance metrics. To guarantee the reliability requirement, the fixed modulation-based SWIPT transmitter adopts the following transmission strategy:

- When instantaneous Signal-to-Noise-Ratio (SNR) γ is higher than threshold γ_0, the SWIPT transmitter sends the modulated symbols to the SWIPT receiver to simultaneously satisfy its information and energy requests.
- When the instantaneous SNR, γ, is lower than the threshold, γ_0, the SWIPT transmitter does not send any modulated symbols to the SWIPT receiver. Therefore, in these instances, the SWIPT system is in the outage. The SWIPT receiver can neither receive any information nor harvest any energy.

Therefore, we can guarantee that either the instantaneous BER or the average BER is lower than the corresponding requirement. Moreover, γ_0 is defined as the transmission switching threshold.

3.1. WIT performance

At the SWIPT transmitter, the modulated symbol is denoted as $x(t)$, having a zero mean and a variance of $E[|x(t)|^2] = 1$, where $E[\cdot]$ and $|\cdot|$ represent the statistical expectation on a random variable and the absolute value of a complex number, respectively. We assume that the average transmit power of the SWIPT transmitter is P_t. All modulated symbols in a constellation of a specific modulation scheme constitute a set $\mathcal{X}$. The i-th modulated symbol $x_i \in \mathcal{X}$ has a probability of p_i to be sent by the SWIPT transmitter, while its transmit power is P_i. Both p_i and P_i satisfy the following equalities:

$$\sum_{i=1}^{M} p_i = 1, \ \sum_{i=1}^{M} p_i P_i = P_t \tag{2}$$

Moreover, by assuming $p_i = \frac{1}{M}$ for $\forall i = 1, \ldots, M$, we have

$$\frac{1}{M} \sum_{i=1}^{M} P_i = P_t \tag{3}$$

In Eqs. (2) and (3), $M = |\mathcal{X}|$ represents the total number of possible modulated symbols in the set $\mathcal{X}$, which is the order of a specific modulation scheme.

We assume that the power splitting ratio of the SWIPT receiver is ρ_{PS}, which means that a portion $\sqrt{\rho_{PS}}$ of the received RF signal is used for energy harvesting, and a portion $\sqrt{1-\rho_{PS}}$ is used for information demodulation. In the k-th symbol duration, the received baseband signal for information demodulation is expressed as

$$y_{ID}[k] = h[k] \sqrt{\frac{(1-\rho_{PS})P_t}{d^{\lambda}}} x[k] + n_{ID}[k] \tag{4}$$

where $n_{ID}[k] \sim \mathcal{N}(0, \sigma_{ID}^2)$ is the additive Gaussian distributed noise. For convenience, we will omit the index k in the rest of the derivations.

We focus on the spectrum efficiency and BER performance of the WIT. As we consider a modulation scheme having an order of M, we cannot exploit the classic Shannon-Hartley's capacity for characterizing the spectrum efficiency of the WIT. This is because Shannon-Hartley capacity is derived by conceiving Gaussian distributed signals having infinite alphabets. Since the input signal is finite and discrete, we turn to the mutual information of discrete-input-continuous-output channels for characterizing the spectrum efficiency of the WIT [26]. The mutual information between the discrete finite channel input, X, and the continuous infinite channel output, Y_{ID}, can be expressed as

$$I(X; Y_{ID}) = \sum_{x \in \mathcal{X}} \int_{-\infty}^{+\infty} p(y_{ID}|x) p(x) \log \frac{p(y_{ID}|x)}{\sum_{x' \in \mathcal{X}} p(y_{ID}|x') p(x')} dy_{ID} \tag{5}$$

where we have the conditional pdf $p(y_{ID}|x)$ expressed as

$$p(y_{ID}|x) = \frac{1}{\sqrt{2\pi\sigma_{ID}^2}} \exp\left(-\frac{(y_{ID} - x)^2}{2\sigma_{ID}^2} \right) \tag{6}$$

for $\forall x \in \mathcal{X}$. According to Ref. [27], the mutual information $I(X; Y_{ID})$ can be maximized when $p(x) = \frac{1}{M}$ for $\forall x \in \mathcal{X}$. However, by substituting $p(x) = \frac{1}{M}$ and $p(y_{ID}|x)$ of Eq. (6) into Eq. (5), we cannot obtain the closed-form mutual information $I(X; Y_{ID})$ due to the existence of the integration. Fortunately, a tight upper-bound for $I(X; Y_{ID})$ has been found by Baccarelli et al. [28], which is expressed as

$$C_M(\gamma) = \log_2 M - \frac{1}{M} \times \sum_{x \in \mathcal{X}} \log_2 \left[1 + (M-1) \exp\left(-\frac{\gamma}{M-1} \sum_{x' \in \mathcal{X}} |x - x'|^2 \right) \right] \tag{7}$$

In Eq. (7), the SNR, γ, of the information demodulator is formulated as

$$\gamma = \frac{v(1-\rho_{PS})P_t}{d^{\lambda}\sigma_{ID}^2} \tag{8}$$

Based on Eqs. (1) and (8), the pdf of the SNR, γ, is obtained as

$$f(\gamma) = \frac{(\gamma/a)^{m-1} m^m \exp(-m\gamma/a)}{a\Gamma(m)} \tag{9}$$

where m is a positive integer, $a = \frac{(1-\rho_{PS})P_t}{d^{\lambda}\sigma_{ID}^2}$. Therefore, the average spectrum efficiency can be formulated as

$$\tilde{C}_M = \int_0^{\infty} C_M(\gamma) f(\gamma)\, d\gamma \tag{10}$$

The actual WIT spectrum efficiency by conceiving the above transmission strategy is reformulated as

$$C_M = \int_{\gamma_0}^{\infty} C_M f(\gamma)\, d\gamma \tag{11}$$

Apart from spectrum efficiency, we should also evaluate the BER performance, when a specific modulation scheme is adopted. According to Ref. [29], the instantaneous BER with respect to the SNR, γ, is formulated as

$$BER_M(\gamma) = \begin{cases} \frac{2(M-1)}{M\log_2 M} Q\left(\sqrt{\frac{6\gamma}{M^2-1}}\right) & \text{for M-PAM} \\ \frac{2}{\log_2 M} Q\left(\sqrt{\gamma}\sin \pi/M\right) & \text{for M-PSK} \\ \frac{4}{\log_2 M} Q\left(\sqrt{\frac{3\gamma}{M-1}}\right) & \text{for M-QAM} \end{cases} \tag{12}$$

where the classic Q-function is expressed as

$$Q(x) = \int_x^{+\infty} \frac{\exp(-0.5t^2)}{\sqrt{2\pi}}\, dt \tag{13}$$

As a result, the average BER over all possible values of random SNR γ is formulated as

$$B\,ER_M = \frac{\int_{\gamma_0}^{\infty} BER_M(\gamma) f(\gamma)\, d\gamma}{\int_{\gamma_0}^{\infty} f(\gamma)\, d\gamma} \tag{14}$$

3.2. WPT performance

Let P_r represent the power of the RF signal for energy harvesting. We consider a linear RF-DC converter, where a constant η represents the linear RF-DC energy conversion efficiency. Without any loss of generality, we assume normalized symbol duration. Hence, by considering the minimum energy P_{th} required for information demodulation, the effective energy harvested can be expressed as

$$P_{EH} = \eta(P_r - P_{th})^+ \tag{15}$$

where $(\cdot)^+$ represents the operation of taking the maximum value between 0 and the input parameter.

After being split by the signal splitter in the power domain, as portrayed in Fig. 2, the RF signal for energy harvesting is expressed as

$$y_{EH} = h\sqrt{\frac{\rho_{PS}P_t}{d^{\lambda}}}x + n_{EH} \tag{16}$$

where n_{EH} is the remaining noise after the signal splitter.

By assuming that a modulated symbol $x_i \in \mathcal{X}$ is sent by the SWIPT transmitter according to Eqs. (8), (15), and (16), the energy harvested by the SWIPT receiver can be formulated as

$$P_{EH}(x_i, \gamma) = \eta\left(\frac{\rho_{PS}P_i\gamma\sigma_{ID}^2}{(1-\rho_{PS})P_t} - P_{th}\right)^+ \tag{17}$$

As the power of n_{EH} is negligibly small, we do not consider it in Eq. (17). According to Ref. [30], the transmit power, P_i, carried by a specific modulated symbol is expressed as

$$P_i = \begin{cases} \frac{3P_t}{M^2-1}\left(3\left\lceil\left|i - \frac{M+1}{2}\right|\right\rceil - 1\right)^2 & \text{M-PAM} \\ P_t & \text{M-PSK} \\ \frac{3P_t}{2(M-1)}\left[\left(2\left\lceil\left|\left\lceil\frac{i}{\sqrt{M}}\right\rceil - \frac{\sqrt{M}-1}{2}\right|\right\rceil\right)^2\right. & \\ \left. + \left(\left\lceil mod(i, \sqrt{M}) - \frac{\sqrt{M}-1}{2}\right\rceil - 1\right)^2\right] & \text{M-QAM} \end{cases} \tag{18}$$

for $\forall i = 1, \ldots, M$, where $\lceil\cdot\rceil$ finds the minimum integer higher than the input parameter and $mod(\cdot, \cdot)$ represents operation of the first input parameter modulo the second. With the aid of Eqs. (17) and (18), and by considering the transmission strategy of the SWIPT transmitter, the average energy harvested by the SWIPT receiver is formulated as

$$P_{EH,M} = \frac{1}{M}\sum_{i=1}^{M}\int_{\gamma_0}^{\infty} P_{EH}(x_i, \gamma) f(\gamma)\, d\gamma \tag{19}$$

which is derived by assuming equal probabilities for all the modulated symbols, namely, $p_i = \frac{1}{M}$ for $\forall i$.

3.3. Transceiver optimization

To achieve a balance among the WIT spectrum efficiency, C_{PS}, of Eq. (11), the average BER, $B\,ER_M$, of Eq. (14), and the average energy harvested, $P_{EH,M}$, of Eq. (19), the SWIPT transceiver optimization problem is formulated as

$$(\text{P1}): \max_{\rho_{PS}, P_t, \gamma_0} C_M \tag{20}$$

$$\text{s. t. } P_{EH,M} \geq P_{EH,0} \tag{20a}$$

$$B\,ER_M \leq BER_0 \tag{20b}$$

$$0 \leq P_t \leq P_{ave} \tag{20c}$$

$$0 \leq \rho_{PS} \leq 1 \tag{20d}$$

This problem maximizes the effective spectrum efficiency C_M by optimizing the power splitting ratio, ρ_{PS}, the transmit power, P_t, of the SWIPT transmitter, and the transmission switching threshold, γ_0. Moreover, the constraint (20a) represents that the average energy harvested, $P_{EH,M}$, should be higher than a threshold $P_{EH,0}$; however, the constraint (20b) represents that the average BER, $B\,ER$, should be lower than a minimum requirement BER_0. Furthermore, as expressed in the constraint (20c), the average transmit power, P_t, should be lower than a threshold P_{ave}, while the power splitting ratio, ρ_{PS}, is a real number between 0 and 1.

By substituting Eq. (14) into the constraint (20b), we obtain a function $\varphi(\gamma_0)$ with respect to γ_0 as

$$\varphi(\gamma_0) = \int_{\gamma_0}^{\infty} BER(\gamma) f(\gamma)\, d\gamma - BER_0 \int_{\gamma_0}^{\infty} f(\gamma)\, d\gamma \leq 0 \tag{21}$$

whose derivative is expressed as

$$\frac{d\varphi(\gamma_0)}{d\gamma_0} = [BER(\gamma_0) - BER_0]\varphi(\gamma_0) \tag{22}$$

By letting $BER_0 = BER(\gamma_0)$, we may find the corresponding $\gamma_0 = \gamma_0^{'}$. According to Eq. (12), $BER(\gamma_0)$ is a decreasing function with respect to its input parameter γ_0. Therefore, by observing the derivative (22), when $\gamma_0 \in (0, \gamma_0^{'})$, $\varphi(\gamma_0)$ is an increasing function, whereas it is a decreasing function if $\gamma_0 \in [\gamma_0^{'}, +\infty)$. Hence, if we let $\gamma_0 = \gamma_0^{'}$, $\varphi(\gamma_0)$ achieves its maximum value 0. If we require the instantaneous BER, $BER(\gamma)$, lower than BER_0 for $\forall\gamma$, we choose the transmission threshold, γ_0, to be $\gamma_0^{'}$. However, in (P1), we consider the average BER constraint, as shown in (20b), and the optimal switching threshold γ_0^* should be within the region $\gamma_0 \in (0, \gamma_0^{'})$, which can be found by a one-dimensional search.

According to Eqs. (7) and (17)-(19), the average spectrum efficiencies, C_M and $P_{EH,M}$, are both increasing functions with respect to the average transmit power, P_t, of the SWIPT transmitter. Moreover, $P_{EH,M}$ is an increasing function with respect to ρ_{PS}, while C_M is a decreasing function with respect to ρ_{PS}. Therefore, based on the above analysis, letting $P_t = P_{ave}$ and $P_{EH,M} = P_{EH,0}$ may return us the optimal transmit power $P_t^* = P_{ave}$ and the optimal power splitting ratio ρ_{PS}^*. Substituting $P_t^* = P_{ave}$ and ρ_{PS}^* into (P1), we may obtain the optimal transmission switching threshold γ_0^* for maximizing the average spectrum efficiency. The pseudo code for solving (P1) is detailed in Algorithm 1, whose complexity is $\mathcal{O}(\log_2(n))$.

Algorithm 1. Fixed modulation based SWIPT transceiver design with an average BER constraint

Algorithm 1 Fixed modulation based SWIPT transceiver design with an average BER constraint

Input: All physical parameters P_{ave}, $P_{EH,0}$, and BER_0 related to the SWIPT transceiver, the path-loss parameters d, λ, and the fading parameter, m, as well as the convergence thresholds, ξ_1 and ξ_2;

Output: Maximum average spectrum efficiency $\overline{C}_M^*$, optimal power splitting ratio ρ_{PS}^*, optimal transmission switching threshold γ_0^*, and optimal transmit power P_t^*.

Initialize $\rho_{PS,\max} \leftarrow 1$, $\rho_{PS,\min} \leftarrow 0$, $\overline{P}_{EH,M} \leftarrow 0$, $\overline{P}_{EH,M,last} \leftarrow -100$;
while $|\overline{P}_{EH,M} - \overline{P}_{EH,M,last}| > \xi_1$ **do**
  Update $\rho_{PS,mid} \leftarrow (\rho_{PS,\max} + \rho_{PS,\min})/2$;
  Update $\rho_{PS}^* \leftarrow \rho_{PS,mid}$;
  Initialize $\gamma_{0,\min} = 0$, $\gamma_{0,\max} \leftarrow \gamma_0^{'}$, $\varphi(\gamma_0) \leftarrow 0$, $\varphi_{last}(\gamma_0) \leftarrow 100$;
  while $|\varphi(\gamma_0) - \varphi_{last}(\gamma_0)| > \xi_2$ **do**
    Update $\gamma_0 \leftarrow (\gamma_{0,\min} + \gamma_{0,\max})/2$;
    if $\varphi(\gamma_0) > 0$ **then**
      Update $\gamma_{0,\min} \leftarrow \gamma_0$;
    else if $\varphi(\gamma_0) < 0$ **then**
      Update $\gamma_{0,\max} \leftarrow \gamma_0$;
    else
      Break from this loop;
    end if
    Update $\varphi_{last}(\gamma_0) \leftarrow \varphi(\gamma_0)$;
  end while
  if $\overline{P}_{PS} > P_0$ **then**
    Update $\rho_{PS,\max} \leftarrow \rho_{PS,mid}$;
  else if $\overline{P}_{PS} < P_0$ **then**
    Update $\rho_{PS,\min} \leftarrow \rho_{PS,mid}$;
  else
    Break from this loop;
  end if
  Update $\overline{P}_{EH,M,last} \leftarrow \overline{P}_{EH,M}$;
end while
Return $\gamma_0^* \leftarrow \gamma_0$, ρ_{PS}^*, $P_t^* \leftarrow P_{ave}$ and the corresponding $\overline{C}_M^*$.

4. Transceiver optimization for adaptive modulation

The spectrum efficiency, BER, and energy-harvesting performance of an adaptive modulation-based SWIPT transceiver will be formulated in this section. Then, to achieve a balance among these conflicting performance measures, an optimal transceiver design is created. The adaptive modulation-based SWIPT transmitter uses the following transmission approach to increase the attainable spectrum efficiency:

- When the instantaneous SNR, γ, is lower than the threshold, γ_0, the SWIPT transmitter does not send any modulated symbols to the SWIPT receiver. Therefore, the SWIPT system is in the outage state in these instances, as portrayed in Fig. 3. The SWIPT receiver can neither receive any information nor harvest any energy.
- According to their various SWIPT performances, the SWIPT transmitter is capable of adaptively switching among QAM family of \{4-QAM, 16-QAM, 64-QAM, 256-QAM, ⋯ \} without any loss of generality. As illustrated in Fig. 3, when the effective SNR for information demodulation falls in a specific region, the digital modulator of the SWIPT transmitter switches to a certain modulation scheme. For instance, M-QAM (simply represented by its order M) is adopted by the digital modulator when the effective SNR is within a region of $[\gamma_{(\log_2 M)/2-1}, \gamma_{(\log_2 M)/2}]$ for $\forall M \in \{4, 16, 64, 256, \ldots, M_{\max}\} \triangleq \mathcal{M}$.
- Since the modulation schemes available for the digital modulator are finite, the highest order of the QAM is $M_{\max}$. When the effective SNR, γ, is higher than $\gamma_{(\log_2 M_{\max})/2-1}$, the $M_{\max}$-QAM is always adopted for modulating the information bits, which means $\gamma_{(\log_2 M_{\max})/2} = +\infty$.

4.1. WIT performance

When M-QAM is selected at the SWIPT transmitter and the power splitter with a ratio ρ_{PS} is adopted at the SWIPT receiver, the attainable spectrum efficiency, C_M, can be then evaluated by Eq. (7). However, this evaluation is only valid when the effective SNR γ satisfies $\gamma \in [\gamma_{(\log_2 M)/2-1}, \gamma_{(\log_2 M)/2}]$. Hence, the average spectrum efficiency can be formulated as

$$\hat{C} = \sum_{M\in\mathcal{M}} \int_{\gamma_{(\log_2 M)/2-1}}^{\gamma_{(\log_2 M)/2}} C_M f(\gamma) d\gamma \tag{23}$$

where $f(\gamma)$ is the PDF of the effective SNR, γ, expressed as Eq. (9).

Apart from the average spectrum efficiency, the reliability of the WIT with adaptive modulation needs to be characterized. Given an instantaneous effective SNR γ, the BER $BER_M(\gamma)$ of M-QAM can be calculated by the third line of Eq. (12). Therefore, by considering the adaptive modulation, the average BER can be formulated as

$$\hat{BER} = \frac{\sum_{M\in\mathcal{M}} \int_{\gamma_{(\log_2 M)/2-1}}^{\gamma_{(\log_2 M)/2}} BER_M(\gamma) f(\gamma) d\gamma}{1 - \int_0^{\gamma_0} f(\gamma) d\gamma} \tag{24}$$

The denominator in Eq. (24) ensures that the outage state is not included in the calculation of the average BER.

4.2. WPT performance

As different modulation schemes are selected within different effective SNR regions, the energy harvesting performance of the SWIPT receiver varies. When the effective SNR, γ, falls in the region of $[\gamma_{(\log_2 M)/2-1}, \gamma_{(\log_2 M)/2}]$, M-QAM is adopted by the SWIPT transmitter, and the average amount of energy harvested by the SWIPT receiver is formulated as

$$\hat{P}_{EH,M} = \frac{1}{M} \sum_{i=1}^{M} \int_{\gamma_{(\log_2 M)/2-1}}^{\gamma_{(\log_2 M)/2}} P_{EH}(x_i, \gamma) f(\gamma) d\gamma \tag{25}$$

where $P_{EH}(x_i, \gamma)$ given by Eq. (17) represents the amount of energy

harvested, when the symbol $x_i(\forall i = 1, \ldots, M)$ is transmitted by the SWIPT transmitter. Note that $\hat{P}_{EH,M}$ is obtained by assuming that all the modulated symbols have equal probabilities to be transmitted. Moreover, the total average amount of energy harvested by the SWIPT receiver is expressed as

$$\hat{P}_{EH} = \sum_{M\in\mathcal{M}} \hat{P}_{EH,M} = \sum_{M\in\mathcal{M}} \frac{1}{M} \sum_{i=1}^{M} \int_{\gamma_{(\log_2 M)/2-1}}^{\gamma_{(\log_2 M)/2}} P_{EH}(x_i,\gamma) f(\gamma) d\gamma \tag{26}$$

4.3. Transceiver optimization

According to the transmission strategy of the adaptive modulation-based SWIPT transmitter, the modulation switching thresholds can be represented by the following vector:

$$\boldsymbol{\gamma} = \left(\gamma_0, \gamma_1, \ldots, \gamma_{(\log_2 M)/2-1}, \cdots, \gamma_{(\log_2 M_{\max})/2-1}\right) \tag{27}$$

Therefore, the adaptive modulation-based transceiver design is formulated by the following optimization problem:

$$\text{(P2):} \quad \max_{\rho_{PS}, P_t, \boldsymbol{\gamma}} \hat{C}_{PS} \tag{28}$$

$$\text{s. t.} \quad \hat{P}_{EH} \geq P_{EH,0} \tag{28a}$$

$$BER(\gamma) \leq BER_0 \quad \text{or} \quad \hat{BER} \leq BER_0 \tag{28b}$$

$$0 \leq P_t \leq P_{ave} \tag{28}$$

$$0 \leq \rho_{PS} \leq 1 \tag{28d}$$

As shown in Eq. (28), the objective of (P2) is to maximize the average spectrum efficiency of the SWIPT system by optimizing the power splitting ratio, ρ_{PS}, of the SWIPT receiver, as well as the modulation-switching thresholds, $\boldsymbol{\gamma}$, and the transmit power, P_t, of the SWIPT transmitter. The constraint (28a) represents that the average amount of energy harvested by the SWIPT receiver has to exceed a minimum requirement, $P_{EH,0}$. Moreover, $BER(\gamma) \leq BER_0$ in the constraint (28b) requires that the instantaneous $BER(\gamma)$ has to be lower than the BER requirement BER_0. It can be relaxed to an average BER constraint of $\hat{BER} \leq BER_0$, which means the BER constraint, BER_0, can be occasionally violated, but the long-term average BER constraint has to be satisfied.

4.3.1. Instantaneous BER constraint

First, we consider the instantaneous BER constraint $BER(\gamma) \leq BER_0$ in (28b). According to Eq. (12), the BER is a decreasing function with respect to the instantaneous effective SNR, γ. Therefore, we investigate the boundary SNR threshold for every member of the QAM family \{4-QAM, 16-QAM, 64-QAM, 256-QAM, $\cdots$ \}, above which the corresponding QAM is capable of satisfying the instantaneous BER constraint, BER_0. Specifically, by letting $BER_M(\gamma^{\dagger}_{(\log_2 M)/2-1}) = BER_0$ of Eq. (12), a feasible boundary SNR threshold $\gamma_{(\log_2 M)/2-1}\dagger$ for the M-QAM is derived as

$$\gamma^{\dagger}_{(\log_2 M)/2-1} = \frac{M-1}{3}\left[Q^{-1}\left(\frac{BER_0 \log_2 M}{4}\right)\right]^2 \tag{29}$$

where $Q^{-1}(\cdot)$ is the inverse Q-function. As the order M increases, the BER performance becomes poorer, given a specific instantaneous effective SNR γ. Similarly, we may get the boundary threshold, $\gamma^{\dagger}_{(\log_2 M)/2}$, for the $(M+1)$-QAM. If the instantaneous effective SNR γ exceeds $\gamma^{\dagger}_{(\log_2 M)/2}$, the $(M+1)$-QAM satisfies the instantaneous BER constraint, BER_0. Moreover, the $(M+1)$-QAM has a higher spectrum efficiency than M-QAM. The digital modulator may adaptively select $(M+1)$-QAM for maximizing the average spectrum efficiency of Eq. (28). Therefore, a range of feasible boundary thresholds $\boldsymbol{\gamma}^{\dagger}$ can be decided, which characterize the operational SNR region of the QAM schemes.

Based on a similar analysis of the SWIPT transceiver design for the fixed modulation, we may obtain the optimal average transmit power as $P_t^{\dagger} = P_{ave}$. A feasible power splitting ratio $\rho_{PS}^{\dagger}$ is derived by solving the equation of $\hat{P}_{EH} = P_{EH,0}$. Therefore, (P2) with a instantaneous BER constraint can be solved by a bisection method, as detailed in Algorithm 2.

Algorithm 2. Adaptive modulation-based transceiver design with an instantaneous BER constraint

Algorithm 2 Adaptive modulation-based transceiver design with an instantaneous BER constraint

Input: All physical parameters and the convergence thresholds, ξ;

Output: Maximum average spectrum efficiency $\widehat{C}_{PS}^{\dagger}$, optimal power splitting ratio $\rho_{PS}^{\dagger}$, optimal modulation switching thresholds $\boldsymbol{\gamma}^{\dagger}$, and optimal transmit power $P_t^{\dagger}$.

Initialize $\rho_{PS,\max} \leftarrow 1$, $\rho_{PS,\min} \leftarrow 0$, $\widehat{P}_{EH} \leftarrow 0$, $\widehat{P}_{EH,last} \leftarrow -100$;
Obtain $\boldsymbol{\gamma}^{\dagger}$ by invoking Eq. (29)
while $|\widehat{P}_{EH} - \widehat{P}_{EH,last}| > \xi_1$ **do**
  Update $\rho_{PS,mid} \leftarrow (\rho_{PS,\max} + \rho_{PS,\min})/2$;
  Update $\rho_{PS}^{\dagger} \leftarrow \rho_{PS,mid}$;
  if $\widehat{P}_{EH} > P_{EH,0}$ **then**
    Update $\rho_{PS,\max} \leftarrow \rho_{PS,mid}$;
  else if $\widehat{P}_{EH} < P_{EH,0}$ **then**
    Update $\rho_{PS,\min} \leftarrow \rho_{PS,mid}$;
  else
    Break from this loop;
  end if
  Update $\widehat{P}_{EH,last} \leftarrow \widehat{P}_{EH}$;
end while
Return $\boldsymbol{\gamma}^{\dagger}$, $\rho_{PS}^{\dagger}$, $P_t^{\dagger} \leftarrow P_{ave}$ and the corresponding $\widehat{C}_{PS}^{\dagger}$.

4.3.2. Average BER constraint

We consider the average BER constraint $\widehat{BER} \leq BER_0$ in (28b). According to Eqs. (23), (24) and (26), transmitting the RF signals with the highest average power $P_t^{\ddagger} = P_{ave}$ may achieve the optimal spectral efficiency, BER, and total energy harvested. However, given non-closed-form expressions on all of these performance metrics and given their non-monotonicity with respect to the power splitting ratio, ρ_{PS}, and the modulation switching thresholds, $\boldsymbol{\gamma}$, the optimal transceiver design problem (P2) with the average BER constraint cannot be solved efficiently with polynomial time complexity. Therefore, a genetic algorithm is invoked for solving this generalized optimization problem, which is detailed in Algorithm 3.

Algorithm 3. Adaptive modulation-based transceiver design with an instantaneous BER constraint

Algorithm 3 Adaptive modulation-based transceiver design with an instantaneous BER constraint

Input: All physical parameters, the convergence thresholds, ξ, the maximum number of generations, G, the population of a single generation, N, mutation probability ϵ, and mutation distance σ;

Output: Maximum average spectrum efficiency $\widehat{C}_{PS}^{\ddagger}$, optimal power splitting ratio $\rho_{PS}^{\ddagger}$, optimal modulation switching thresholds $\boldsymbol{\gamma}^{\ddagger}$, and optimal transmit power $P_t^{\ddagger}$.

1: Randomly initialise a generation $\mathcal{G} \leftarrow \{(\boldsymbol{\gamma}_{(j)}, \rho_{PS,(j)}) | j = 1, \cdots, N\}$ with a population of N. All the randomly generated variables are within their definitional domains.
2: Initialise a generation index $g \leftarrow 1$, $\widehat{C}_{PS}^{\ddagger} \leftarrow 0$, and $\widehat{C}_{PS,last}^{\ddagger} \leftarrow 2\xi$;
3: **while** $|\widehat{C}_{PS}^{\ddagger} - \widehat{C}_{PS,last}^{\ddagger}| > \xi$ & $g \leq G$ **do**
4: Obtain $\{(\widehat{C}_{PS,(j)}, \widehat{P}_{EH,(j)}, \widehat{BER}_{(j)}) | j = 1, \cdots, N\}$ by substituting all the population of the g-th generation $\mathcal{G}$ into Eqs. (23), (24) and (26);
5: Update $\widehat{C}_{PS,(j)} \leftarrow -\infty$, if either $\widehat{P}_{EH,(j)} < P_{EH,0}$ or $\widehat{BER}_{(j)} > BER_0$, for $\forall j = 1, \cdots, N$;
6: Obtain the survival probabilities $\left\{p_{s,(j)} \leftarrow \frac{\widehat{C}_{PS,(j)}}{\sum_j \widehat{C}_{PS,(j)}} | \forall j = 1, \cdots, N\right\} \triangleq \mathbf{p}_s$;
7: **if** $\max_j\{\widehat{C}_{PS,(j)}\} > \widehat{C}_{PS}^{\ddagger}$ **then**
8: Update $\widehat{C}_{PS,last}^{\ddagger} \leftarrow \widehat{C}_{PS}^{\ddagger}$, $\widehat{C}_{PS}^{\ddagger} \leftarrow \max_j\{\widehat{C}_{PS,(j)}\}$, $j^{\ddagger} \leftarrow \arg\max_j\{\widehat{C}_{PS,(j)}\}$ and $(\boldsymbol{\gamma}^{\ddagger}, \rho_{PS}^{\ddagger}) \leftarrow (\boldsymbol{\gamma}_{(j^{\ddagger})}, \rho_{PS,(j^{\ddagger})})$;
9: **end if**
10: **Natural Selection**: Randomly select individuals from $\mathcal{G}$ to constitute parents set $\mathcal{G}_{sel}$, according to the survival probabilities $\mathbf{p}_s$;
11: **if** $\mathcal{G}_{sel}$ is null **then**
12: **Mutation:** Update $\mathcal{G}$ by letting $\{(\boldsymbol{\gamma}_{(j)} \leftarrow \boldsymbol{\gamma}_{(j)} + z_{\gamma}, \rho_{PS,(j)} \leftarrow \rho_{PS,(j)} + z_{\rho}) | j = 1, \cdots, N\}$, where $z_{\gamma}, z_{\rho} \sim \mathcal{N}(0, \sigma^2)$;
13: Truncate $\mathcal{G}$ to satisfy the definitional domains of all its elements;
14: **else**
15: **Crossover:** Obtain $\mathcal{G}' \triangleq \left\{(\boldsymbol{\gamma}'_{(j)}, \rho'_{PS,(j)}) \leftarrow \frac{(\boldsymbol{\gamma}'_{(q)}, \rho'_{PS,(q)}) + (\boldsymbol{\gamma}_{(l)}, \rho_{PS,(l)})}{2} | \forall j = 1, \cdots, N\right\}$, where $(\boldsymbol{\gamma}'_{(q)}, \rho'_{PS,(q)})$ and $(\boldsymbol{\gamma}'_{(l)}, \rho'_{PS,(l)})$ are individuals randomly chosen from the parents set $\mathcal{G}_{sel}$;
16: **Mutation:** Each element in $\mathcal{G}'$ has a probability of ϵ to be mutated as Line 12; $\mathcal{G}'$ also needs to be truncated;
17: Update $\mathcal{G} \leftarrow \mathcal{G}'$;
18: **end if**
19: **end while**
20: Return $\boldsymbol{\gamma}^{\ddagger}, \rho_{PS}^{\ddagger}, P_t^{\ddagger} \leftarrow P_{ave}$ and the corresponding $\widehat{C}_{PS}^{\ddagger}$.

5. Numerical results

The fixed and adaptive modulation-based SWIPT transceiver generally obeys the following parameter settings without further descriptions. The transmit distance is $d = 10$ m, while the path loss exponent is set to $\lambda = 3$. The fading parameter is $m = 1$ and the RF-DC conversion efficiency is set to $\eta = 0.5$. The average transmit power of the SWIPT transmitter is set to $P_{ave} = 10$ dBm, while the noise power of the information demodulator is $\sigma_{ID}^2 = -50$ dBm. The energy consumption of the SWIPT receiver is $P_{th} = -20$ dBm. The maximum BER that can be tolerated by the SWIPT receiver is set to $BER_0 = 10^{-4}$.

5.1. Fixed modulation

First, we study the SWIPT performance of different modulation schemes with a fading factor of $m = 1$. Fig. 4 shows that the M-PAM scheme performs better when M is low. However, if we increase M to 16, M-QAM outperforms M-PAM and M-PSK. As portrayed in Fig. 4, M-PAM outperforms M-PSK and M-QAM when the minimum energy-harvesting requirement, $P_{EH,0}$, is very high. Furthermore, a modulation scheme having a higher order achieves a higher spectrum efficiency, when the minimum energy-harvesting requirement, $P_{EH,0}$, is in a low region. However, if we continuously increase $P_{EH,0}$, the modulation schemes having $M = 4$ achieve the highest spectrum efficiency. We then investigate the SWIPT performance of a high-order modulation scheme. Fig. 4 shows that 256-QAM has the poorest SWIPT performance. This is because 256-QAM has the worst reliability performance. To satisfy the BER requirement, the SWIPT transmitter has to stay in the outage state, which substantially reduces the spectrum efficiency and energy-harvesting performance.

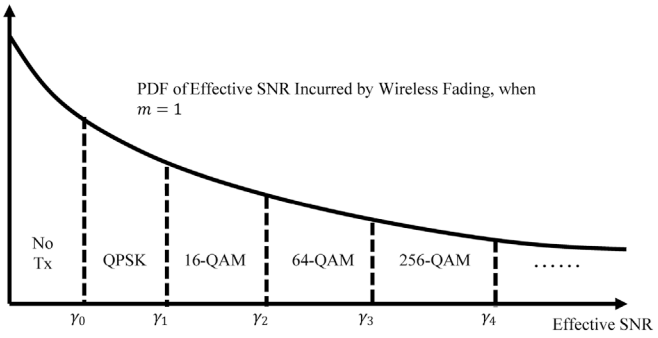

Fig. 3. Different modulation schemes with different orders.

Second, we study the effect of fading channel on the SWIPT performance in Fig. 5, where the fading factor is set to $m = \{1, 5, 10\}$. Fig. 5 shows that when $m = 10$, which represents a less fading channel, the spectrum efficiency of all the modulation schemes is higher than that of $m = 1$, which represents a more fading channel. However, in a less fading channel associated with $m = 10$, the energy harvested by the SWIPT receiver is much lower than a fading channel having $m = 1$. This observation provides meaningful insight for deploying SWIPT in different channel conditions. The WIT performance is better in a less fading channel. By contrast, since a more fading channel provides plenty of multi-path transmissions, the accumulated signal received at the SWIPT receiver has a higher chance of exceeding the energy-harvesting threshold, P_{th}, which results in a better WPT performance.

Third, we investigate the effect of energy harvesting threshold, P_{th}, on the SWIPT performance of different modulation schemes with a fading factor of $m = 1$, where we have $P_{th} = 0$ (no threshold) and $P_{th} = -20$ dBm. Fig. 6 shows that when $P_{th} = 0$, 16-QAM performs best in terms of SWIPT performance, followed by 16-PSK and 16-PAM in descending order. In contrast, when we have $P_{th} = -20$ dBm, 16-QAM performs best. However, 16-PSK may achieve a higher spectrum efficiency than 16-PAM in a low region of the minimum energy harvesting requirement, $P_{EH,0}$. In a high region of $P_{EH,0}$, 16-PAM performs better than 16-PSK. Furthermore, when we do not have any threshold effect in energy harvesting, all modulation schemes have a substantially higher SWIPT performance than a non-zero threshold P_{th}.

Finally, we study the effect of different BER requirements on the SWIPT performance in Fig. 7, where we have $BER_0 = 10^{-4}$ as the black curves and $BER_0 = 10^{-2}$ as the red curves. Fig. 7 shows that when we have $BER_0 = 10^{-2}$, the SWIPT performance of all the modulation schemes is higher than that of $BER_0 = 10^{-4}$. This is because when we have a strict BER requirement, the SWIPT transmitter may frequently be in the outage state, which substantially reduces the spectrum efficiency and energy-harvesting performance. Furthermore, we compare the SWIPT performance of practical modulation schemes associated with a finite alphabet to the Gaussian distributed signals. The big gap in terms of the SWIPT performance between Gaussian signals and practical modulations tells us that Gaussian signals are meaningless in the future deployment of the SWIPT system. Instead, we have to consider actual signalling with practical modulations.

5.2. Adaptive modulation

In Fig. 8, we show the SWIPT performance of the adaptive modulation-based transceiver and its fixed modulation-based equivalents with the immediate and average BER constraints. When the instantaneous and average BER limitations are equivalent to $BER_0 = 10^{-4}$, adaptive modulation can achieve a substantially bigger rate-energy region than other fixed modulation systems, as demonstrated in Fig. 8(a) and (b).

Specifically, as shown in Fig. 8(a), we consider an instantaneous BER constraint. When the minimum power requirement of the energy harvesting is 0.5 μW, the 64-QAM-based transceiver achieves a rate of 3.6 bits/channel use, which is the highest among all the fixed modulation schemes. However, the adaptive modulation is capable of achieving a rate of 5.1 bits/channel use, which is almost 50% higher than the 64-QAM-based counterpart. Moreover, given a certain rate of 3 bits/channel use, the energy harvesting performance of the 16-QAM is 1.3 μW, which is the highest among all the fixed counterparts. However, the adaptive modulation is capable of achieving 1.7 μW, which is 31% higher than the 16-QAM. Note that the performance of the fixed modulation-based transceiver with an instantaneous BER constraint is obtained by invoking Algorithm 2, when a single modulation scheme is conceived.

Similar performance gains of adaptive modulation over the fixed counterparts can be observed in Fig. 8(b), when an average BER constraint is considered. For example, when a specific energy-harvesting power requirement 0.5 μW is considered, the adaptive modulation can achieve 6.5 bits/channel use, which is 51% higher than the 64-QAM. Furthermore, when a rate of 3 bits/channel is specified, adaptive modulation can attain an energy-harvesting performance of 2.32 W, which is 55% greater than 16-QAM. Furthermore, by comparing the simulation results in Fig. 8(a) and (b), we can see that imposing an average BER limit effectively expands the rate-energy region.

6. Practicality and insights

Our model and analysis are based on a practical digital communication system for SWIPT that is reflected by the following aspects:

- We consider practical modulation schemes with finite numbers, such as M-QAM, rather than theoretical Gaussian signalling.
- We consider practical Discrete Input Continuous Output (DICO) mutual information to evaluate WIT performance, rather than Shannon capacity by assuming Gaussian-distributed continuous channel input.
- We consider a Nakagami-m fading channel to characterize different fading conditions. For example, $m = 1$ represents Rayleigh fading without LoS, while an increasing m represents an increasing portion of LoS.

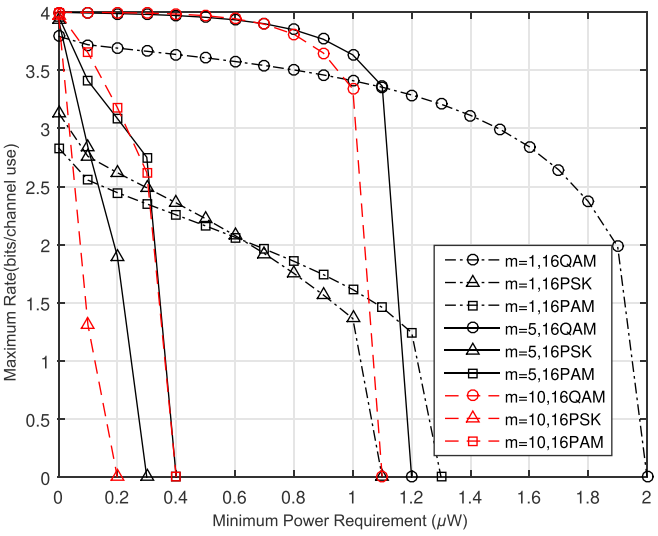

Fig. 5. Different modulation schemes with different fading channel.

Therefore, considering the above-mentioned practicality, we may obtain the following insights from our analysis:

- Different modulation schemes have distinct SWIPT performance, as introduced in Section 2.1. Specifically, a higher order of the modulation scheme has a better WPT performance when we have a higher energy-harvesting threshold P_{th}. Otherwise, a lower order of modulation scheme may achieve a better WPT performance. This analysis motivates us to design an adaptive modulation scheme for achieving a better SWIPT performance.
- The DICO mutual information of an M-QAM scheme converges to M bits/channel use as we continuously increase the SNR of the information decoder. This indicates that we do not need to let more received RF signals flow to the information decoder, as this may not linearly increase the WIT performance when we design the power

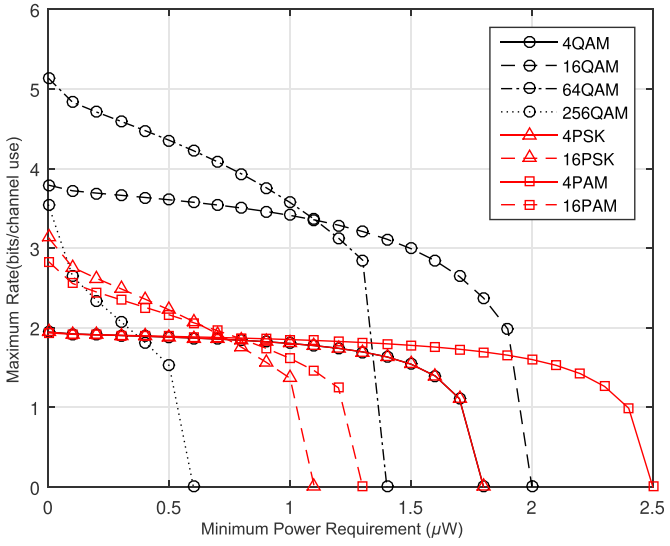

Fig. 4. Different modulation schemes with different orders.

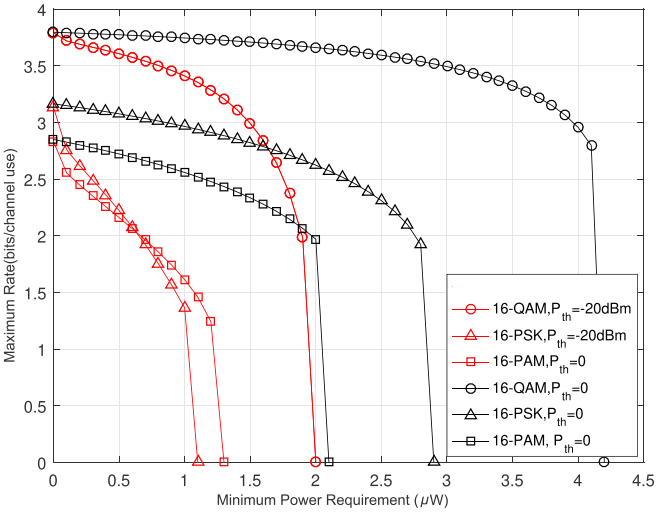

Fig. 6. Different modulation with two energy harvesting threshold.

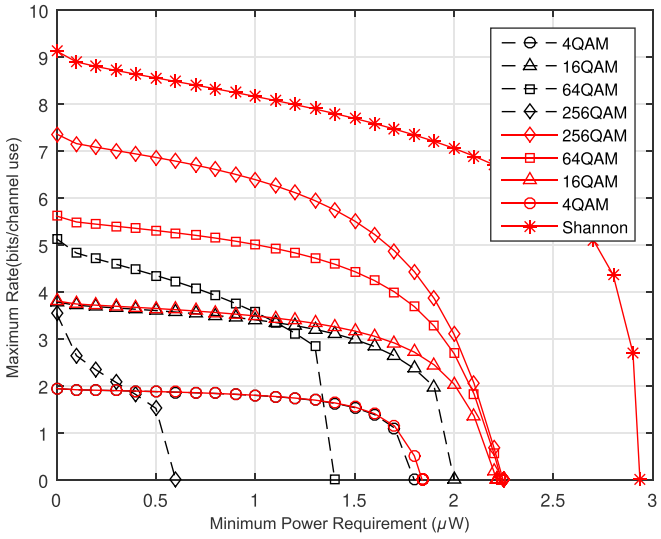

Fig. 7. M-QAM with different BER requirements.

splitter. When the WIT performance converges, we should let more received RF signals to the energy harvester to further increase the WPT performance.

- A lower m represents a more severe multipath fading condition, which harms the WIT performance but improves the WPT performance. This is because in a more severe multipath fading condition, the signals propagating along these paths may have a good chance to be constructively combined at the receiver. Therefore, the total received signal has a higher Peak-to-Average Power Ratio (PAPR), which is beneficial for increasing the WPT performance.

Imperfect channel estimation does affect the performance of the proposed adaptive modulation scheme. According to Ref. [31], the average BER of the M-QAM based adaptive modulation scheme can only tolerate the channel estimation error with a Mean Square Error (MSE) lower than − 25 dB. However, in practical applications of SWIPT, the distance between the SWIPT transmitter and receiver should not be higher than 15 m to ensure that sufficient energy can be harvested. By considering the simulation settings in Section 5, the modulation switching thresholds are obtained as 12, 18, 24, and 30 dB, as shown in Fig. 8(b), when the minimum energy-harvesting requirement is 1.5 μW. According to Fig. 8 of [32], the MSE of the channel estimation is approximately − 36 dB by exploiting a linear minimum mean square error-based channel estimation scheme when the SNR is 12 dB. When the SNR increases, the MSE can be further reduced. When the MSE is lower than −36 dBm, the average BER and other SWIPT performance are no longer sensitive to the channel estimation error in practice. As a result, for the practical application of SWIPT, we think the imperfect CSI might not be a problem for our proposed adaptive modulation scheme.

7. Conclusions

In this study, we investigated the SWIPT performance of practical modulation schemes with finite alphabets. We used fixed and adaptive modulation schemes to optimize the SWIPT transceiver's WIT spectrum efficiency while meeting energy-harvesting and reliability criteria. We came to some crucial conclusions based on our numerical findings: 1) with a practical energy harvester, M-PAM outperforms M-PSK and M-QAM in terms of WPT. M-QAM, on the contrary, outperforms both M-PAM and M-PSK in terms of WIT performance; 2) a more fading channel is bad for WIT but good for WPT; 3) the large SWIPT performance gap between ideal Gaussian signaling and practical modulations indicates that practical modulation-based signaling should be considered in future SWIPT system design; and 4) the adaptive modulation can substantially increase both the spectrum efficiency and the total energy harvested, given a specific BER constraint.

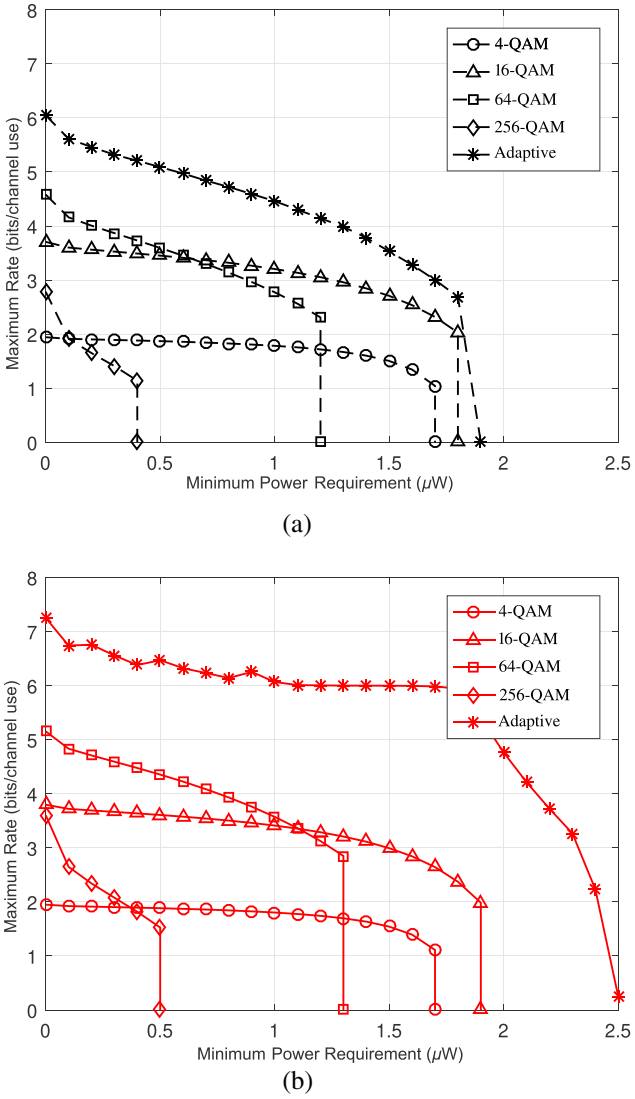

Fig. 8. Adaptive modulation-based transceiver versus fixed modulation-based counterpart with (a) instantaneous BER constraint and (b) average BER constraint. The adaptive modulation-based SWIPT transmitter chooses a modulation scheme from 4-QAM, 16-QAM, 64-QAM, and 256-QAM.

Declaration of competing interest

The authors declare that they have no known competing financial interests or personal relationships that could have appeared to influence the work reported in this paper.

Acknowledgement

The authors would like to thank the financial support of National Natural Science Foundation of China (NSFC), Grant No. 61 971 102, 61 871 076 and the Key Research and Development Program of Zhejiang Province under Grant No. 2022C01093.

References

[1] Toh C.K., Security for smart cities[J]. IET Smart Cities 2 (2) (2020) 95–104.
[2] Y. Zhao, J. Hu, K. Yang and S. Cui, "Deep Reinforcement Learning Aided Intelligent Access Control in Energy Harvesting Based WLAN," in IEEE Transactions on Vehicular Technology, vol. 69, no. 11, pp. 14078-14082, Nov. 2020.
[3] B.H. Choi, V.X. Thai, E.S. Lee, J.H. Kim, C.T. Rim, Dipole-coil-based wide-range inductive power transfer systems for wireless sensors, IEEE Trans. Ind. Electron. 63 (5) (2016) 3158–3167.
[4] V. Jiwariyavej, T. Imura, Y. Hori, Coupling coefficients estimation of wireless power transfer system via magnetic resonance coupling using information from either side of the system, IEEE J. Emerg. Sel. Top. Power Electron. 3 (1) (2015) 191–200.
[5] J. Hu, K. Yang, G. Wen, L. Hanzo, Integrated data and energy communication network: a comprehensive survey, IEEE Commun. Surv. Tutorials 20 (4) (2018) 3169–3219.
[6] W. Saad, M. Bennis, M. Chen, A vision of 6G wireless systems: applications, trends, technologies, and open research problems, IEEE Netw. 34 (3) (2020) 134–142.
[7] Y. Zhao, J. Hu, R. Guo, K. Yang and S. Leng, "Enhanced CSMA/CA Protocol Design for Integrated Data and Energy Transfer in WLANs," 2018 IEEE Global Communications Conference (GLOBECOM), 2018, pp. 1-6.
[8] J. Hu, X. Cai and K. Yang, "Joint Trajectory and Scheduling Design for UAV Aided Secure Backscatter Communications," in IEEE Wireless Communications Letters, vol. 9, no. 12, pp. 2168-2172, Dec. 2020.
[9] B. Clerckx, Wireless information and power transfer: nonlinearity, waveform design, and rate-energy tradeoff, IEEE Trans. Signal Process. 66 (4) (2018) 847–862.
[10] R.F. Buckley, R.W. Heath, System and design for selective OFDM SWIPT transmission, IEEE Trans. Green Commun. Netw. (2020), 1–1.
[11] L. Dai, B. Wang, M. Peng, S. Chen, Hybrid precoding-based millimeter-wave massive MIMO-NOMA with simultaneous wireless information and power transfer, IEEE J. Sel. Area. Commun. 37 (1) (2019) 131–141.
[12] Q. Yue, J. Hu, K. Yang, C. Huang, Transceiver design for simultaneous wireless information and power multicast in multi-user mmWave MIMO system, IEEE Trans. Veh. Technol. 69 (10) (2020) 11394–11407.
[13] K. Lv, J. Hu, Q. Yu, K. Yang, Throughput maximization and fairness assurance in data and energy integrated communication networks, IEEE Internet Things J. 5 (2) (2018) 636–644.
[14] Y. Zhao, J. Hu, Y. Diao, Q. Yu, K. Yang, Modelling and performance analysis of wireless LAN enabled by RF energy transfer, IEEE Trans. Commun. 66 (11) (2018) 5756–5772.
[15] Y. Zhao, D. Wang, J. Hu, K. Yang, H-AP deployment for joint wireless information and energy transfer in smart cities, IEEE Trans. Veh. Technol. 67 (8) (2018) 7485–7496.
[16] I.-M. Kim, D.I. Kim, Wireless information and power transfer: rate-energy tradeoff for equi-probable arbitrary-shaped discrete inputs, IEEE Trans. Wireless Commun. 15 (6) (2016) 4393–4407.
[17] X. Zhu, W. Zeng, C. Xiao, Precoder design for simultaneous wireless information and power transfer systems with finite-alphabet inputs, IEEE Trans. Veh. Technol. 66 (10) (2017) 9085–9097.
[18] B. Chen, X. Zhu, X. Tu, Joint precoder design for SWIPT-enabled MIMO relay networks with finite-alphabet inputs, IEEE Access 8 (2020) 179105–179117.
[19] J. Hu, Y. Zhao, K. Yang, Modulation and coding design for simultaneous wireless information and power transfer, IEEE Commun. Mag. 57 (5) (2019) 124–130.
[20] E. Bayguzina, B. Clerckx, Asymmetric modulation design for wireless information and power transfer with nonlinear energy harvesting, IEEE Trans. Wireless Commun. 18 (12) (2019) 5529–5541.
[21] Y. Zhao, J. Hu, Z. Ding, K. Yang, Joint interleaver and modulation design for multi-user SWIPT-NOMA, IEEE Trans. Commun. 67 (10) (2019) 7288–7301.
[22] Y. Zhao, J. Hu, A. Xie, K. Yang, K.-K. Wong, Receive spatial modulation aided simultaneous wireless information and power transfer with finite alphabet, IEEE Trans. Wireless Commun. 19 (12) (2020) 8039–8053.
[23] J. Hu, L. Zhang, Q. Yu, K. Yang, Wireless information and energy provision with practical modulation in energy self-sustainable wireless networks, in: Proceedings of IEEE MSN, vol. 2020, 2020.
[24] A. Svensson, An introduction to adaptive QAM modulation schemes for known and predicted channels, Proc. IEEE 95 (12) (2007) 2322–2336.
[25] J. Hu, L. Yang, L. Hanzo, Maximum average service rate and optimal queue scheduling of delay-constrained hybrid cognitive Radio in Nakagami fading channels, IEEE Trans. Veh. Technol. 62 (5) (2013) 2220–2229.
[26] G. Xia, Y. Lin, X. Zhou, W. Zhang, F. Shu, J. Wang, Hybrid precoding design for secure generalized spatial modulation with finite-alphabet inputs, IEEE Trans. Commun. (2020), 1–1.
[27] R. Zhang, L.-L. Yang, L. Hanzo, Error probability and capacity analysis of generalised pre-coding aided spatial modulation, IEEE Trans. Wireless Commun. 14 (1) (2015) 364–375.
[28] E. Baccarelli, A. Fasano, Some simple bounds on the symmetric capacity and outage probability for QAM wireless channels with Rice and Nakagami fadings, IEEE J. Sel. Area. Commun. 18 (3) (2000) 361–368.
[29] A. Goldsmith, Wireless Communications, Cambridge University Press, 2005.
[30] M.K. Simon, M.S. Alouini, Digital Communication over Fading Channels: A Unified Approach to Performance Analysis, Wiley, 2000.
[31] J. Paris, M. Aguayo-Torres, J. Entrambasaguas, Impact of channel estimation error on adaptive modulation performance in flat fading, IEEE Trans. Commun. 52 (5) (2004) 716–720.
[32] V. Savaux, F. Bader, Y. Louët, A joint MMSE channel and noise variance estimation for OFDM/OQAM modulation, IEEE Trans. Commun. 63 (11) (2015) 4254–4266.